

# Parabenzoquinone Pyrolysis and Oxidation in a Flow Reactor

MARIA U. ALZUETA,<sup>1</sup> MIRIAM OLIVA,<sup>2</sup> PETER GLARBORG<sup>3</sup>

<sup>1,2</sup>Department of Chemical and Environmental Engineering, University of Zaragoza, Centro Politécnico Superior. María de Luna, 3, 50015 Zaragoza, Spain

<sup>3</sup>Department of Chemical Engineering, Technical University of Denmark, 2800 Lyngby, Denmark

Received 29 September 1997; accepted 7 April 1998

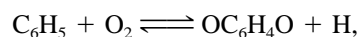
**ABSTRACT:** An experimental and theoretical study of the pyrolysis and oxidation of parabenzoquinone has been performed. The experiments were conducted in an isothermal quartz flow reactor at atmospheric pressure in the temperature range 600–1500 K. The main variables considered are temperature, oxygen concentration, and presence of CO. A detailed reaction mechanism for the pyrolysis and oxidation chemistry of parabenzoquinone is proposed, which provides a good description of the experimental results. Both the experimental work and the kinetic mechanism proposed for the pyrolysis and oxidation of parabenzoquinone represent the first systematic study carried out for this important aromatic compound.

Our pyrolysis results confirm that the primary dissociation channel for *p*-benzoquinone leads to CO and a C<sub>5</sub>H<sub>4</sub>O isomer, presumably cyclopentadienone. However, significant formation of CO<sub>2</sub> during the pyrolysis may indicate the existence of a secondary dissociation channel leading to CO<sub>2</sub> and a C<sub>5</sub>H<sub>4</sub> isomer. Under oxidizing conditions, consumption of *p*-benzoquinone occurs mainly by dissociation at lower temperatures. As the temperature increases interaction of OC<sub>6</sub>H<sub>4</sub>O with the radical pool becomes more significant, occurring primarily through hydrogen abstraction reactions followed by ring opening reactions of the OC<sub>6</sub>H<sub>3</sub>O radical. © 1998 John Wiley & Sons, Inc. *Int J Chem Kinet*: 30: 683–697, 1998

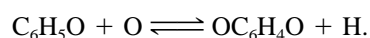
## INTRODUCTION

Understanding of the detailed oxidation chemistry of aromatic compounds is still a major challenge. Despite significant efforts during the last two decades [1–9] large uncertainties remain in the reaction mechanism for even the simplest aromatic species, such as benzene. While the initial steps in benzene oxidation are now better understood [4–6, 8–11], little is known

about some of the intermediates formed during the oxidation process. A number of recent studies have pointed to the importance of benzoquinone, OC<sub>6</sub>H<sub>4</sub>O, which appears to be an important product in the reaction between phenyl and oxygen [12,13],



and may also be formed by reaction of the phenoxy radical with oxygen atoms [14],



In addition to being an important intermediate in benzene oxidation, benzoquinone has been identified as a potential pollutant from combustion facilities such as

Correspondence to: M. U. Alzueta

Contract grant Sponsor: Department of Chemical and Environmental Engineering of the University of Zaragoza and Department of Chemical Engineering of the Technical University of Denmark (CHEC). The CHEC research program is cofunded by the Danish Technical Research Council, Elsam, Elkraft, and the Danish Ministry of Energy

© 1998 John Wiley & Sons, Inc.

CCC 0538-8066/98/090683-15

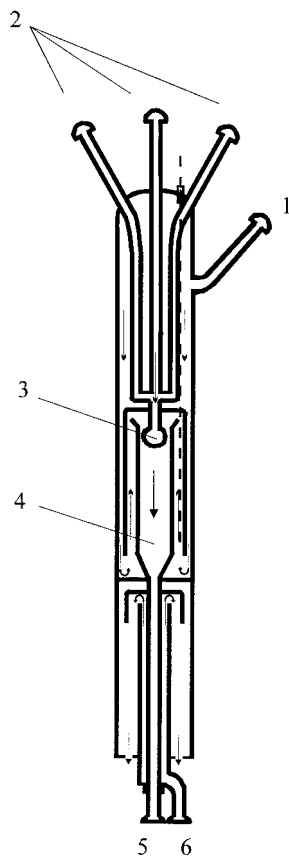


**Figure 1** Diagram of the quartz-flow reactor. 1: Main flow. 2: Gas injectors. 3: Mixing area. 4: Reaction zone. 5: Gas outlet. 6: Cooling air inlet.

sewage sludge incinerators [15]. Despite the potential importance of benzoquinone, very little is currently known about the chemistry of this component. Two isomers of benzoquinone may be of significance, parabenzoquinone ( $p$ -OC<sub>6</sub>H<sub>4</sub>O, in this article just termed OC<sub>6</sub>H<sub>4</sub>O), and orthobenzoquinone ( $o$ -OC<sub>6</sub>H<sub>4</sub>O). It is not clear at present which form of benzoquinone is favored in the C<sub>6</sub>H<sub>5</sub> + O<sub>2</sub> and C<sub>6</sub>H<sub>5</sub>O + O reactions, but it is likely that both isomers play a role [16,17].

A limited amount of experimental data on the chemistry of benzoquinone can be found in the literature. The only reaction specific work reported is a shock-tube pyrolysis study of parabenzoquinone by Frank et al. [12]. Further studies on  $p$ -benzoquinone include flash-thermolysis experiments [18–20] and thermal-hydrogenation experiments [21–25]. For  $o$ -benzoquinone, to our knowledge only thermolysis data have been reported [26,27]. While the reported studies on benzoquinone have provided important information on the pyrolysis chemistry, no data are available on the oxidation behavior. Furthermore, except for the shock-tube study, none of these experiments have

been performed under well-defined reaction conditions, making it difficult to derive reaction specific information.

It appears that the two isomers of benzoquinone have different reaction characteristics, even though little mechanistic information is available. Flash thermolysis of the two isomers at temperatures around 1100 K [18,19,26,27] indicate that the pyrolysis of  $p$ -benzoquinone and  $o$ -benzoquinone may proceed along fundamentally different pathways, perhaps because different C<sub>5</sub>H<sub>4</sub>O isomers are formed in the initial pyrolysis step [18,19]. Parabenzoquinone is more thermally stable [12] than orthobenzoquinone, which has been reported to dissociate readily [26,28]. This is in agreement with the general observation that  $o$ -quinones are decarbonylated more readily than  $p$ -quinones [23].

The objective of the present work is to perform an experimental and theoretical study of parabenzoquinone pyrolysis and oxidation. Experiments are conducted in a flow reactor in the temperature range from 600 to 1500 K at atmospheric pressure. Based on the present data as well as results from the literature, a detailed reaction mechanism for the chemistry of parabenzoquinone is proposed, that provides a good description of the experimental results under both pyrolysis and oxidation conditions.

## EXPERIMENTAL

The experimental installation basically consists of a gas-feeding system, a gas-reaction system, and a gas-analysis system. Pure gases from gas cylinders are dosed with mass-flow controllers and fed into the reactor. The addition of  $p$ -benzoquinone together with water vapor was done by passing a nitrogen stream through a saturated solution of  $p$ -benzoquinone at a temperature of 303 K.

The reaction system contains a quartz-flow reactor which is located inside an electrically heated oven that allows us to reach temperatures up to 1500 K. The reactor, which has been constructed following the design of Kristensen et al. [29], is shown schematically in Figure 1. It has a reaction zone of 8.7 mm inside diameter and 200 mm in length. Reaction conditions are carefully controlled. The reactants are led separately to the reactor and rapidly and efficiently mixed at the entrance of the reaction zone. The temperature is kept uniform along the reaction zone within 7 K.

The gas entering into the reaction zone consists of a mixture of  $p$ -benzoquinone, water vapor, and nitrogen, with oxygen added in the oxidation experiments. The reactants are very diluted in order to keep iso-

thermal conditions along the reaction zone. At the outlet of the reactor, the reaction is quenched using cooling air.

The analysis of the products after conditioning is performed by means of continuous analyzers for CO and CO<sub>2</sub>, with an estimated uncertainty of the measurements of 5%, but not less than 5 ppm. Furthermore, the products are analyzed using a FTIR (Fourier Transform Infra-Red) analyzer. The reactor temperature is measured with a K thermocouple, and the pressure with an absolute pressure transducer. Temperature control and data acquisition are performed in a PC system.

## REACTION MECHANISM

The reaction mechanism for benzoquinone pyrolysis and oxidation developed in the present work consists of an oxidation subset for C<sub>3</sub>–C<sub>6</sub> hydrocarbons, listed in Appendix A, together with a C<sub>2</sub> hydrocarbon subset, which includes C<sub>1</sub> hydrocarbon chemistry as well as oxidation of CO/H<sub>2</sub>. The C<sub>2</sub> subset was adopted without changes from Glarborg et al. [30]. The C<sub>3</sub>–C<sub>4</sub> reaction subset was largely taken from work of Miller and co-workers [31,32]. Thermodynamic data were taken from different sources [30,33,34], and Appendix B lists thermodynamic properties ( $\Delta H_{f,298}$ ,  $S_{298}$ , and  $C_p$ ) for selected species. Reactions of benzoquinone and the subsequent C<sub>6</sub> and C<sub>5</sub> intermediates are discussed in detail below.

As stated in the introduction, very little is currently known about the detailed chemistry of benzoquinone. Only pyrolysis and hydrogenation studies have been reported in literature, and results from these studies are not conclusive.

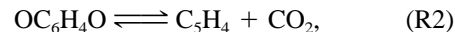
The thermal stability of parabenzoquinone was investigated in a shock-tube study by Frank et al. [12]. The temporal absorption of H, O, and CO was monitored during the unimolecular decomposition of low initial concentrations of *p*-benzoquinone. Frank et al. [12] detected only CO in measurable quantities, with  $[CO]_{\text{end}}/[OC_6H_4O]_0 = 1.0 \pm 0.1$  in the temperature range 1550–1900 K. Based on this information and assuming a high-thermal stability of C<sub>5</sub>H<sub>4</sub>O, they deduced that the reaction



was the only important dissociation channel. From the pseudo-first-order increase of CO, they found a rate constant for (R1) of  $7.4 \cdot 10^{11} \exp(-29700/T) \text{ s}^{-1}$ .

Results of the present work, supported by thermal decarbonylation studies of parabenzoquinone at

860 K in the presence of hydrogen by Sakai and co-workers [21–24], point to a possible different interpretation of the shock-tube results of Frank et al. [12]. We believe that a secondary pyrolysis channel may be active,



with a rate comparable to that of (R1) at high temperatures. This secondary channel was not detected by Frank and co-workers, partly because they did not analyze for the products of (R2) and partly because their assumption of a high-thermal stability of C<sub>5</sub>H<sub>4</sub>O may have been in error. As discussed in detail below, we estimate rate constants for (R1) of  $3.7 \cdot 10^{11} \exp(-29700/T) \text{ s}^{-1}$  and (R2) of  $3.5 \cdot 10^{12} \exp(-33700/T) \text{ s}^{-1}$ , based on pyrolysis results carried out in the present study as well as our interpretation of the results of Sakai et al. and Frank et al. However, the occurrence of reaction (R2), which would involve the formation of a 1,4 bridge of O<sub>2</sub>, is presently only a working hypothesis, and it needs to be confirmed independently.

To our knowledge there are no data available in the literature on reactions of benzoquinone with radicals. The reaction of OC<sub>6</sub>H<sub>4</sub>O with H atoms presumably has two product channels,



For reaction (R3) we have assumed that the H addition to an unsubstituted ring position was rate limiting and we have chosen a rate of four times the value for a position in phenol [35,36]. The H atom may also add to the oxygen in OC<sub>6</sub>H<sub>4</sub>O, which following H atom transfer and subsequent dissociation would result in the same products as (R3). For the H abstraction channel the rate constant was estimated by analogy with the C<sub>6</sub>H<sub>6</sub> + H reaction. Due to the lack of thermodynamic data for the OC<sub>6</sub>H<sub>3</sub>O radical, we have assumed the reactions of this species to be irreversible.

The reaction of benzoquinone with O atoms was also estimated by analogy with the corresponding benzene reaction. The C<sub>6</sub>H<sub>6</sub> + O reaction has two important product channels, one forming a C<sub>6</sub>H<sub>6</sub>O adduct, which yields a phenoxy radical plus an H atom [37], and an H abstraction channel leading to phenyl and OH. By analogy we obtain for the OC<sub>6</sub>H<sub>4</sub>O + O reaction,

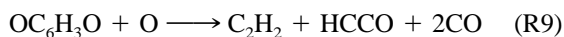


The reaction of parabenzoquinone with OH can be assumed to proceed as an addition reaction at low temperature, similar to the addition to the  $>C=C<$  double bond in 1,4-naphthoquinone [38,39]. However, under the conditions of the present work, the adduct formed presumably dissociates rapidly back to reactants. At higher temperatures we assume that the H abstraction reaction,



is the only active channel. The rate for this reaction can be estimated at 1050–1100 K from the present work (see below), yielding a value of  $1.5 \cdot 10^{11} \text{ cm}^3/\text{mole}\cdot\text{s}$  at 1075 K. We have extrapolated this value, assuming a  $T^2$  dependence. It is noteworthy that the reaction is significantly slower than the  $C_6H_6 + OH$  reaction.

The  $OC_6H_3O$  radical is expected to react very fast with H and O radicals, leading to ring opening



The  $C_6H_3O_3$  radical formed in (R5) with two  $>C=O<$  double bonds and a  $>C-O<$  single bond, presumably has a low-thermal stability; we expect it to dissociate rapidly in the ring opening step,



The fate of  $C_5H_4O$  formed in the primary dissociation step of parabenzoquinone is not certain. There are indications that cyclopentadienone dimerizes fast [28], but results are not conclusive. A flash-thermolysis study at 1580 K by de Champlain and de Mayo [20] identified cyclopentadienone, isolated as the dimer, as the main product. However, at lower temperatures, down to 1420 K, the yield of the dimer progressively decreased. In a similar study performed at 1120 K, Hageman and Wiersum [18,19] failed to detect the cyclopentadienone dimer and concluded that under these conditions a different isomer of ( $C_5H_4O$ ), most likely a cyclopropanone, was the precursor of the major final product, vinylacetylene.

Under the conditions of the present experiments, we believe that the dimerization of  $C_5H_4O$  is too slow to compete with thermal dissociation or reaction with radicals. Our results support the suggestion of Emdee et al. [4], that  $C_5H_4O$  dissociates to  $C_2H_2$  and CO,



with a rate of  $1.0 \cdot 10^{15} \exp(-39300/T) \text{ s}^{-1}$ . Reactions of  $C_5H_4O$  with H and O radicals are expected to lead to ring opening,



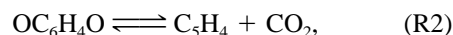
We assume that  $C_5H_4$  formed in reaction (R2) is the noncyclic 1,4 pentadiyne isomer. Reactions of this component with the O/H radical pool presumably proceed as H abstraction reactions producing the  $C_5H_3$  radical, which subsequently may react with  $O_2$  feeding into the  $C_2$  hydrocarbon subset.

## RESULTS AND DISCUSSION

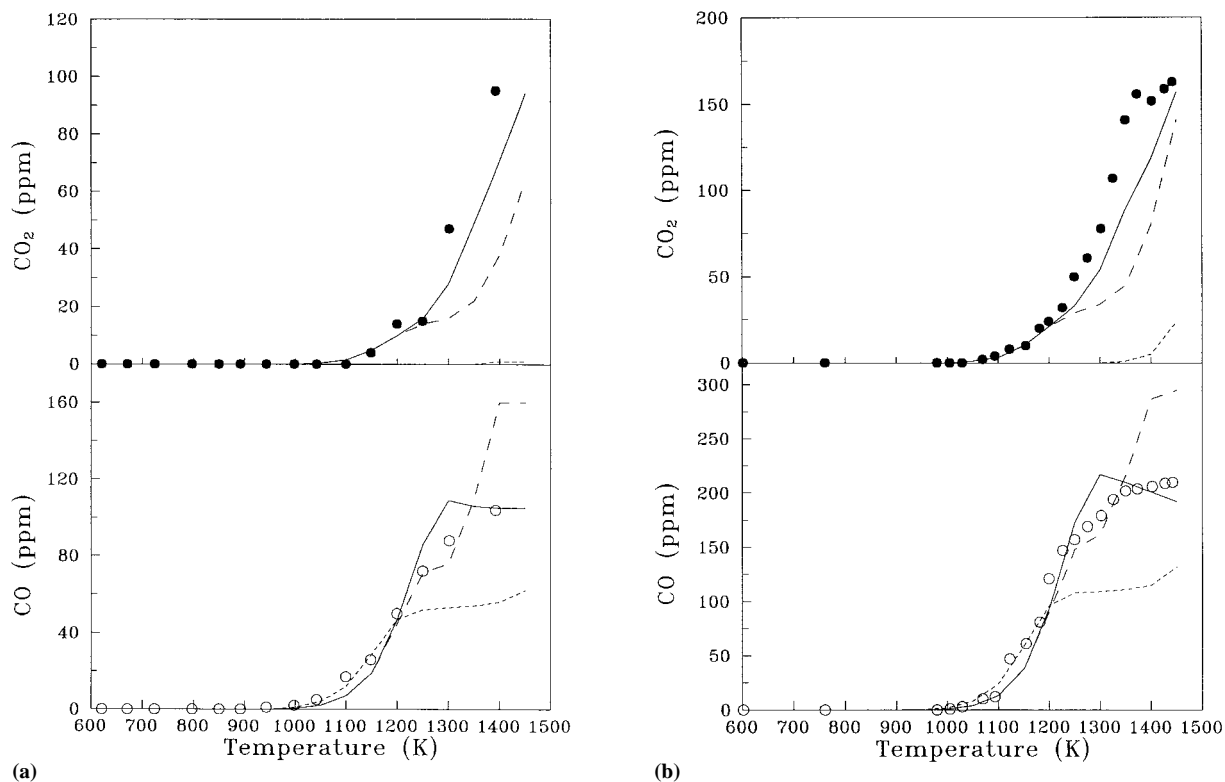
The pyrolysis and oxidation of *p*-benzoquinone has been studied in the temperature range 600–1500 K at atmospheric pressure in a flow reactor. The experiments were conducted keeping a constant mass flow rate and varying the reaction temperature. This means that the residence time in the reactor is a function of temperature, being about 200 ms at 1000 K. The model calculations were performed using Senkin [40], a plug-flow code that runs in conjunction with the Chemkin library [41].

### Pyrolysis of *p*-Benzoquinone

The key issues in the pyrolysis of parabenzoquinone are the branching fraction between the two potential dissociation channels,



and the fate of  $C_5H_4O$  formed in reaction (R1). Frank et al. [12] proposed, based on high-temperature shock-tube results for *p*-benzoquinone dissociation, that (R1) is the dominating dissociation channel, and that cyclopentadienone is thermally very stable. Hydrogenation studies by Sakai and co-workers [21–24] at 860 K confirm that CO is the dominating pyrolysis product, but also significant amounts of  $CO_2$  were observed. Sakai et al. [22,24] suggest that the  $CO_2$  is formed by an intramolecular mechanism, i.e. (R2), since  $CO_2$  was not observed in the pyrolysis of reactants such as phenol, 1-naphthol, or fluorenone with only one oxygen molecule in their structure and since in the case of 1,4-naphthoquinone pyrolysis, the rate of  $CO_2$  formation was practically independent of the  $H_2$  dilution ratio.



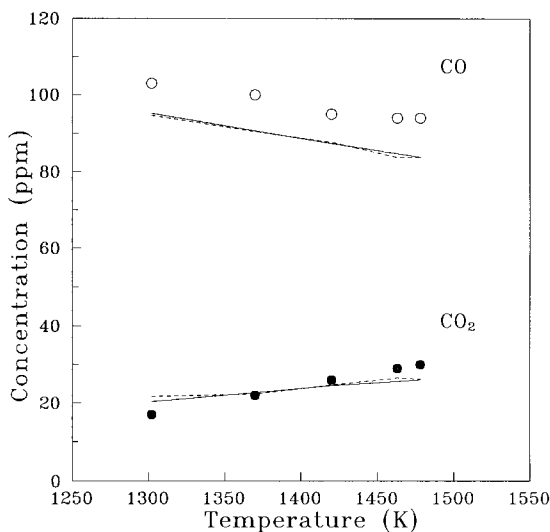
**Figure 2** (a) Comparison of experimental data and model predictions for CO and CO<sub>2</sub> formation in the pyrolysis of *p*-benzoquinone. Symbols denote experimental data and lines denote model predictions. Inlet concentrations: 52 ppm OC<sub>6</sub>H<sub>4</sub>O; 50 ppm O<sub>2</sub>; 2.4% H<sub>2</sub>O; and balance N<sub>2</sub>. Pressure is 1.03 atm. Residence time (s) = 210/T(K). Solid lines: calculations made with the mechanism of the present work (App. A). Short dashed lines: calculations made omitting reaction 2, with the reaction rate recommended by Frank et al for (R1), and with a reaction rate of  $1.0 \cdot 10^{12} \exp(-39300/T)$  for reaction (R12). Long dashed lines: calculations made with a different product channel for reaction (R12), i.e., C<sub>5</sub>H<sub>4</sub>O  $\rightleftharpoons$  CH<sub>2</sub>CHCCH + CO. (b) Inlet concentrations: 108 ppm OC<sub>6</sub>H<sub>4</sub>O; 50 ppm O<sub>2</sub>; 5.1% H<sub>2</sub>O; and balance N<sub>2</sub>. Pressure is 1.03 atm. Residence time (s) = 202/T(K). The rest as in Figure 2(a).

Figure 2(a) and (b) show results from the present study for CO and CO<sub>2</sub> in the pyrolysis of *p*-benzoquinone. Symbols denote experimental results and lines model calculations. The decomposition of *p*-benzoquinone, evidenced by the onset of CO formation, starts slowly at a temperature of approximately 950 K, and becomes faster for temperatures higher than 1100 K. Formation of CO<sub>2</sub> is observed at temperatures above 1050 K, and at 1400 K the amount of CO<sub>2</sub> is comparable to that of CO.

Unfortunately, the interpretation of the results of Figure 2(a) and (b) is complicated by the presence of other sources of CO<sub>2</sub> than reaction (R2). Due to impurities in the N<sub>2</sub> gas cylinders and to the oxygen dissolved in the aqueous solution of *p*-benzoquinone through which the nitrogen stream is saturated, a little amount of oxygen can be present in the experiments. We have estimated the O<sub>2</sub> impurity to be  $50 \pm 10$  ppm. Due to the presence of O<sub>2</sub>, an O/H radical

pool builds up, and CO and other intermediates formed during the pyrolysis may lead to production of CO<sub>2</sub>. The presence of H<sub>2</sub>O may further enhance OH radical formation at high temperatures.

The presence of oxygen in trace concentrations is difficult to avoid experimentally. However, the oxygen impurity is not directly associated with the *p*-benzoquinone feed, and, therefore, the impact of the O<sub>2</sub> impurity will decrease as the concentration of OC<sub>6</sub>H<sub>4</sub>O increases for similar experimental conditions. Unfortunately, it was not possible to assess the significance of the O<sub>2</sub> impurity in this way, because experimentally the *p*-benzoquinone level could not be raised sufficiently. Figure 2(a) and (b) show results with 52 and 108 ppm of OC<sub>6</sub>H<sub>4</sub>O, respectively. At the higher *p*-benzoquinone level (Fig. 2(b)), the CO<sub>2</sub>/OC<sub>6</sub>H<sub>4</sub>O ratio at high temperatures is diminished, suggesting that some of the CO<sub>2</sub> formation can be attributed to the presence of impurities.



**Figure 3** CO and CO<sub>2</sub> concentrations in the pyrolysis of *p*-benzoquinone in presence of excess NH<sub>3</sub>. Symbols denote experimental data and lines denote model predictions. Inlet concentrations: 68 ppm OC<sub>6</sub>H<sub>4</sub>O; 3850 ppm NH<sub>3</sub>; 50 ppm O<sub>2</sub>; 3.8% H<sub>2</sub>O; and balance N<sub>2</sub>. Pressure is 1.03 atm. Residence time (s) = 240/T(K). Solid lines: calculations made with a simplified three reaction model, including OC<sub>6</sub>H<sub>4</sub>O and C<sub>5</sub>H<sub>4</sub>O dissociation (R1, R2, R12). Short dashed lines: calculations made with the mechanism of the present work, plus a subset for NH<sub>3</sub> oxidation, and a rate constant for C<sub>5</sub>H<sub>3</sub> + O<sub>2</sub> (R20) of 1.0 · 10<sup>10</sup>.

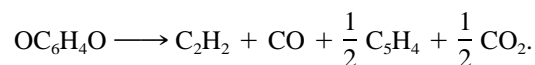
In order to minimize the effect of side reactions leading to CO<sub>2</sub>, a *p*-benzoquinone pyrolysis experiment was carried out in the presence of a large excess of NH<sub>3</sub>. The amines act as a radical sink, reducing the impact of side reactions. The results are shown in Figure 3. As the temperature increases from 1300 to 1480 K, CO<sub>2</sub> increases from 17 ppm to about 30 ppm, i.e., a significant fraction of the benzoquinone input. Still, comparison with the results of Figure 2(a) and (b) shows that the presence of NH<sub>3</sub> suppresses CO<sub>2</sub> formation considerably at higher temperatures. At 1300 K, the [CO<sub>2</sub>]<sub>out</sub>/[OC<sub>6</sub>H<sub>4</sub>O]<sub>in</sub> ratio decreases from 55–70% to 25%, and the effect is even more pronounced at higher temperatures. Furthermore, [CO + CO<sub>2</sub>]<sub>out</sub>/[OC<sub>6</sub>H<sub>4</sub>O]<sub>in</sub> drops from 2.2–2.7 to 1.8 at 1300 K and from 3.4–3.8 to 1.8 at 1400 K.

We have investigated different possible routes to CO and CO<sub>2</sub> formation under the reaction conditions of Figure 3. It is noteworthy that the sum CO + CO<sub>2</sub> remains constant within a few ppm in the whole temperature range of 1300–1480 K in Figure 3. Furthermore, within the experimental uncertainty the sum corresponds to twice the inlet concentration of OC<sub>6</sub>H<sub>4</sub>O. This suggests that formation of CO<sub>*x*</sub> (*x* = 1,2) arises

largely as release of CO/CO<sub>2</sub> from benzoquinone and subsequent ring intermediates; little further oxidation of carbon from the original ring structure takes place.

The recommendation of Frank et al. [12] with only (R1) active as dissociation channel for parabenzoquinone and high-thermal stability for cyclopentadienone leads to a [CO<sub>*x*</sub>]<sub>out</sub>/[OC<sub>6</sub>H<sub>4</sub>O]<sub>in</sub> ratio of 1.0, unless secondary reactions of C<sub>5</sub>H<sub>4</sub>O produces CO/CO<sub>2</sub>. Even with very fast rates, reactions of C<sub>5</sub>H<sub>4</sub>O with the O/H radical pool leads to insufficient formation of CO/CO<sub>2</sub>, due to the low radical concentrations. Another potential consumption channel of C<sub>5</sub>H<sub>4</sub>O is dimerization. The dimerization reaction has been suggested to be an important reaction pathway for cyclopentadienone under pyrolysis and hydrogenolysis conditions [20,28]. In order to explain the observed CO<sub>*x*</sub> formation by this pathway, assuming fast-thermal dissociation of the dimer to produce two CO molecules, a dimerization rate of about 3.0 · 10<sup>10</sup> cm<sup>3</sup>/mole-s is required at 1300 K. From analogy with other Diels–Alder reactions [42] we estimate an upper limit of 1.0 · 10<sup>12</sup>exp(−7550/T) cm<sup>3</sup>/mole-s. This rate constant results in a value of 3.0 · 10<sup>9</sup> cm<sup>3</sup>/mole-s at 1300 K, i.e., too slow to account for the observed results. For this reason, a high-thermal stability of C<sub>5</sub>H<sub>4</sub>O appears to be in disagreement with our experimental results. However, it should be noted that a very fast dimerization rate for C<sub>5</sub>H<sub>4</sub>O, 8.5 · 10<sup>11</sup> cm<sup>3</sup>/mole-s at 850 K, has been suggested in literature [28] and further work is needed in order to resolve this issue.

Reinterpretation of the shock-tube results of Frank et al. [12] in terms of two dissociation channels for parabenzoquinone, (R1) and (R2), with comparable rates, followed by dissociation of C<sub>5</sub>H<sub>4</sub>O, suggests that the measured rate applied to the following global reaction,



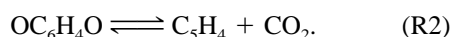
The rate constant for (R1) at high temperatures is, thus, roughly half of that determined by Frank et al. Adopting the activation energy suggested by the shock-tube results, we obtain a rate constant for reaction (R1) of 3.7 · 10<sup>11</sup> exp(−29700/T) s<sup>−1</sup>, which is also the value listed in Appendix A. Based on the results shown in Figure 2(a) and (b) and matching the concentration of CO with the mechanism of Appendix A at 1100 K, where no or very little CO<sub>2</sub> is formed, we obtain a rate for reaction (R1) of 1.9 s<sup>−1</sup> for the results of Figure 2(a) and of 0.9 s<sup>−1</sup> for the results of Figure 2(b). From these data, an optimum value of 1.4 s<sup>−1</sup> for the reaction rate at 1100 K is obtained. Within the uncertainty of

the determination, this value agrees with the  $k_1$  expression adopted in this work.

Routes to  $\text{CO}_2$  other than direct dissociation of parabenzoquinone (R2) were evaluated. Due to the low radical concentrations, little oxidation of CO to  $\text{CO}_2$  is predicted. Assuming that only CO is formed from parabenzoquinone dissociation and that cyclopentadienone further leads to release of CO/ $\text{CO}_2$ , either directly through dissociation and/or reaction with the radical pool or through a fast dimerization, the level of  $\text{CO}_2$  predicted at 1300 K for the conditions of Figure 2(a) is below 1 ppm, i.e., much lower than the observed value of 17 ppm. Direct  $\text{CO}_2$  formation from dissociation of the dimer appears to be unlikely, bearing in mind the structure of the dimer [28].

We also performed a flash-pyrolysis experiment in a laboratory atmospheric fluidized bed reactor at a reaction temperature of  $1085 \pm 10$  K. A flash-pyrolysis experiment of solid *p*-benzoquinone is suitable for determining the CO and  $\text{CO}_2$  distribution when these products are formed, since the solid *p*-benzoquinone fed into the reactor reaches instantaneously the desired reaction temperature. A detailed description of the experimental setup used can be found elsewhere [43]. *P*-benzoquinone particles with a diameter smaller than 0.5 mm were transported into the reactor at a feeding rate of 1–2 g/min, using nitrogen as fluidizing agent with a flow rate of approximately 1000 ml/min. Both CO and  $\text{CO}_2$  were detected and a CO/ $\text{CO}_2$  ratio between 6.1 and 7.5 was found in this experiment.

From this discussion, we suggest that a secondary dissociation channel for parabenzoquinone, leading to  $\text{CO}_2$ , is active, i.e.,



In order to estimate the rate constant for reaction (R2), we have analyzed the results of Figure 3, the results of the flash-pyrolysis experiment, as well as those of the hydrogenation study by Sakai et al. [21–24] at 860 K and the shock-tube study by Frank et al. [12] at 1550–1900 K.

The results of Figure 3 were analyzed partly in terms of the detailed chemistry, partly in terms of a simple three reaction model including only benzoquinone dissociation (reactions (R1) and (R2)) and cyclopentadienone dissociation (R12). In both models, the rate constant for (R1) was the estimate of the present work, i.e., half the value recommended by Frank et al. [12], while  $k_{12}$  was taken from Emdee et al. [4]. The detailed modeling involved two changes compared to the Appendix A mechanism: a  $\text{NH}_3$  reaction subset was included [44], and the rate constant for the  $\text{C}_5\text{H}_3 + \text{O}_2$  reaction was lowered to

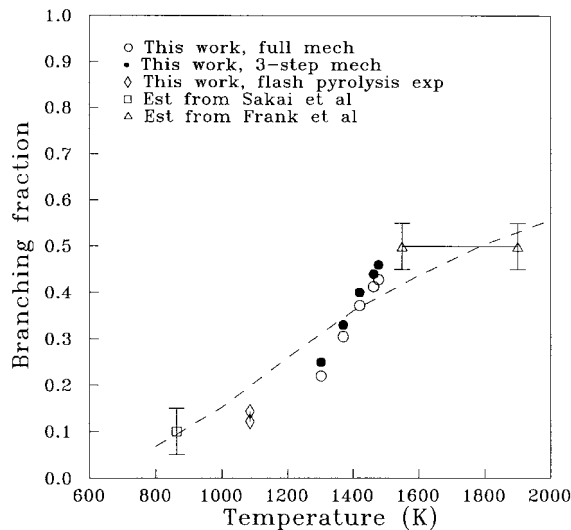


**Figure 4** Branching fraction  $k_2/(k_1 + k_2)$  for dissociation of  $\text{OC}_6\text{H}_4\text{O}$  as a function of temperature. The values associated with the work of Sakai et al. [21–24] and Frank et al. [12] are based on our interpretation of their data, as explained in the text.

$1.0 \cdot 10^{10}$   $\text{cm}^3/\text{mole}\cdot\text{s}$  to avoid prediction of excessive oxidation to CO and  $\text{CO}_2$  at high temperatures. Presumably the  $\text{C}_5\text{H}_3$  radical reacts mainly with the amine pool under the conditions of Figure 3. The FTIR spectra obtained indicate the presence of CN bonds formed from such hydrocarbon/amine interactions.

In the modeling only the  $\text{CO}_2$  formation was considered. For each temperature the value of  $k_2$  was adjusted to obtain the best fit between the predicted value of  $\text{CO}_2$  and the measurement. The results in Figure 4 show the branching fraction  $k_2/(k_1 + k_2)$  as function of temperature. The values obtained with the 3-step model can be considered upper limits for the branching fraction, since pathways to  $\text{CO}_2$  competing with (R2) were neglected. The results obtained with the full mechanism are also uncertain, partly due to the uncertainties in the parabenzoquinone pyrolysis subset, partly because the amine pyrolysis chemistry is not yet well established [45]. However, the results obtained, with a branching fraction increasing from 0.13 at 1085 K, and from 0.25–0.30 at 1300 K to 0.40–0.45 at 1500 K, are in reasonable agreement with the data derived from the hydrogenation study of Sakai et al. and the shock-tube study by Frank et al., as discussed below.

The shock-tube study by Frank et al. [12] showed that in the 1550–1900 K range, only CO was detectable as pyrolysis product (among CO, H, and O), and  $[\text{CO}]_{\text{end}}/[\text{OC}_6\text{H}_4\text{O}]_0 = 1.0 \pm 0.1$ . If the assumption that  $\text{C}_5\text{H}_4\text{O}$  dissociates rapidly compared to  $\text{OC}_6\text{H}_4\text{O}$

at these temperatures is correct, these results indicate that the branching fraction  $\alpha$  is  $0.5 \pm 0.05$  under the conditions of the shock-tube experiments.

The results of Sakai et al. [21–24] must be interpreted with care, partly because the purity of the *p*-benzoquinone was not better than 80–90% and partly because surface reactions may have had some effect. Furthermore, a considerable formation of high molecular weight substances was detected, and these may conceivably also have been a source for  $\text{CO}_2$ . Observations for anthraquinone and phenanthrenequinone [23] indicate that silica-glass surface reactions act to increase the overall conversion rate and may also catalyze the formation of the high molecular compounds. However, the effect of wall reactions on *p*-benzoquinone pyrolysis or hydrogenolysis has not been investigated.

Despite these uncertainties, the rate of formation of CO and  $\text{CO}_2$  in the hydrogenation experiments provides some information of the branching fraction of the parabenzoquinone dissociation. Assuming that reactions other than the two dissociation steps (R1) and (R2) can be neglected as sources of CO and  $\text{CO}_2$  in the early stages of reaction, we derive a value of  $\alpha = 0.10 \pm 0.05$  at 863 K.

Figure 4 summarizes the results on the branching fraction for parabenzoquinone dissociation. From the data we have estimated a rate constant for reaction (R2) of  $3.5 \cdot 10^{12} \exp(-33700/T) \text{ s}^{-1}$ .

The solid lines of Figure 2(a) and (b) denote model calculations with the mechanism proposed in this work (Appendix A). The agreement between model calculations and experimental results is fairly good, even though at high temperatures CO is slightly overpredicted and  $\text{CO}_2$  is somewhat underpredicted. Despite these differences, the model succeeds in predicting the initiation temperature of *p*-benzoquinone thermal decomposition as well as the concentrations up to temperatures of 1250 K.

Our interpretation of the shock-tube parabenzoquinone dissociation data requires that cyclopentadienone dissociates fairly rapidly, releasing CO. The rate and product channel for  $\text{C}_5\text{H}_4\text{O}$  dissociation proposed by Emdee et al. [4], i.e., that the dissociation proceeds as



with a rate of  $1.0 \cdot 10^{15} \exp(-39300/T) \text{ s}^{-1}$ , is in agreement with this interpretation and is supported by the present results, as evidenced by the solid line model predictions in Figure 2(a) and (b).

The short-dashed lines in Figure 2(a) and (b) denote model predictions carried out according to the recommendation of Frank et al., i.e., with a rate constant

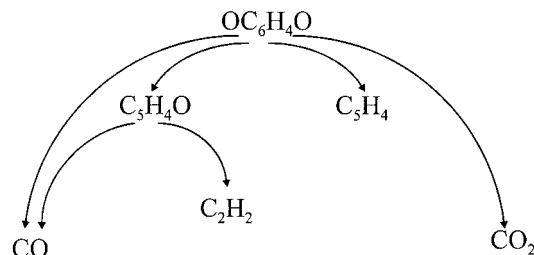


**Figure 5** Reaction path diagram for *p*-benzoquinone pyrolysis.

of  $7.4 \cdot 10^{11} \exp(-29790/T) \text{ s}^{-1}$  for reaction (R1), omitting reaction (R2), and assuming a high-thermal stability for cyclopentadienone, corresponding to a dissociation rate of  $1.0 \cdot 10^{12} \exp(-39300/T) \text{ s}^{-1}$ . To avoid significant CO production from dissociation of  $\text{C}_5\text{H}_4\text{O}$  (below 10% of the total CO formation) under the shock-tube conditions, the rate of (R12) must be three orders of magnitude lower than estimated by Emdee et al. The predictions conducted with these assumptions imply very little formation of  $\text{CO}_2$  and a considerably lower CO formation at temperatures higher than 1150 K than is observed experimentally.

We also tested another product channel for  $\text{C}_5\text{H}_4\text{O}$  dissociation, i.e.,

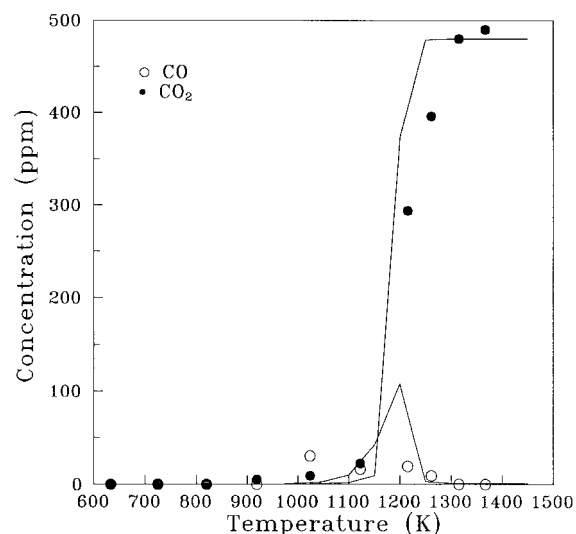


**Figure 6** Comparison of experimental data and model predictions for CO and  $\text{CO}_2$  formation in the oxidation of *p*-benzoquinone. Symbols denote experimental data and lines denote model predictions. Inlet concentrations: 81 ppm  $\text{OC}_6\text{H}_4\text{O}$ ; 0.1%  $\text{O}_2$ ; 1.8%  $\text{H}_2\text{O}$ ; and balance  $\text{N}_2$ . Pressure is 1.03 atm. Residence time (s) =  $240/T(\text{K})$ .

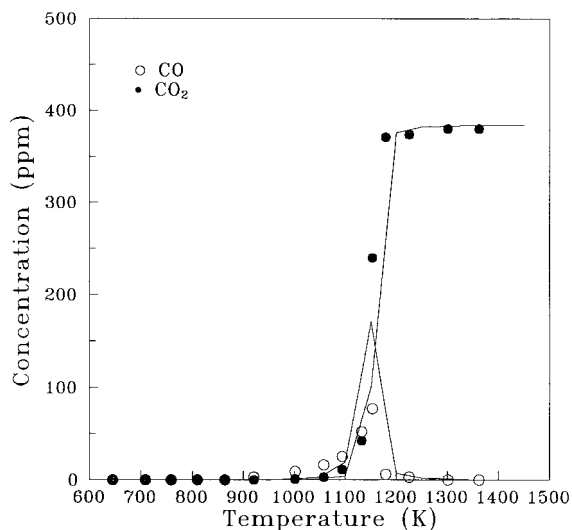


**Figure 7** Comparison of experimental data and model predictions for CO and CO<sub>2</sub> formation in the oxidation of *p*-benzoquinone. Symbols denote experimental data and lines denote model predictions. Inlet concentrations: 64 ppm OC<sub>6</sub>H<sub>4</sub>O; 4.1% O<sub>2</sub>; 1.8% H<sub>2</sub>O; and balance N<sub>2</sub>. Pressure is 1.03 atm. Residence time (s) = 197/T(K).

The results with (R12a) replacing (R12) are shown in Figure 2(a) and (b) as long-dashed lines. At temperatures higher than 1250 K, discrepancies for CO and CO<sub>2</sub> are important, indicating that the product channel suggested by Emdee and co-workers is the most likely. However, uncertainties in the CH<sub>2</sub>CHCCH oxidation subset may partly be responsible for the observed difference, and more work is needed to verify the rate and product channel for cyclopentadienone dissociation.

The importance of the dimerization channel was also investigated. Calculations were performed using

the estimated upper limit for the dimerization reaction ( $1.0 \cdot 10^{12} \exp(-7550/T) \text{ cm}^3/\text{mole}\cdot\text{s}$ ), and assuming the dimer to dissociate thermally to C<sub>6</sub>H<sub>5</sub>C<sub>2</sub>H<sub>3</sub> + 2CO with a rate of  $1.0 \cdot 10^{12} \exp(-30000/T) \text{ s}^{-1}$ . The results roughly coincided with the results obtained with the mechanism listed in Appendix A. Even with the high dimerization rate and assuming irreversible reactions, the dimerization process has little impact under the present experimental conditions.

Figure 5 shows a reaction pathway diagram of *p*-benzoquinone pyrolysis for a temperature of 1050 K, based on the present mechanism. At low temperature, *p*-benzoquinone is mainly consumed through the reaction  $\text{OC}_6\text{H}_4\text{O} \rightleftharpoons \text{C}_5\text{H}_4\text{O} + \text{CO}$  (R1), but as the temperature increases, also the secondary dissociation channel,  $\text{OC}_6\text{H}_4\text{O} \rightleftharpoons \text{C}_5\text{H}_4 + \text{CO}_2$  (R2), becomes important. Cyclopentadienone is mainly consumed by thermal decomposition, leading to acetylene and carbon monoxide. The C<sub>5</sub>H<sub>4</sub> formed through reaction (R2) is thermally stable. In the presence of radicals, caused by the oxygen impurity, C<sub>5</sub>H<sub>4</sub> may by reaction with the O/H radical pool be converted to the C<sub>5</sub>H<sub>3</sub> radical, which presumably feeds into the C<sub>2</sub> hydrocarbon pool.

### Oxidation of *p*-Benzoquinone

Figures 6 and 7 show results for CO and CO<sub>2</sub> obtained in *p*-benzoquinone oxidation experiments with two different oxygen concentrations. The onset of reaction as well as the oxidation of *p*-benzoquinone at lower temperatures are roughly independent of the O<sub>2</sub> concentration. The formation of CO is initiated at a temperature of approximately 1050 K and reaches its maximum concentration at around 1150 K. Above 1250 K all the CO is converted to CO<sub>2</sub>. Even though the oxygen level has little effect on the CO profiles, it

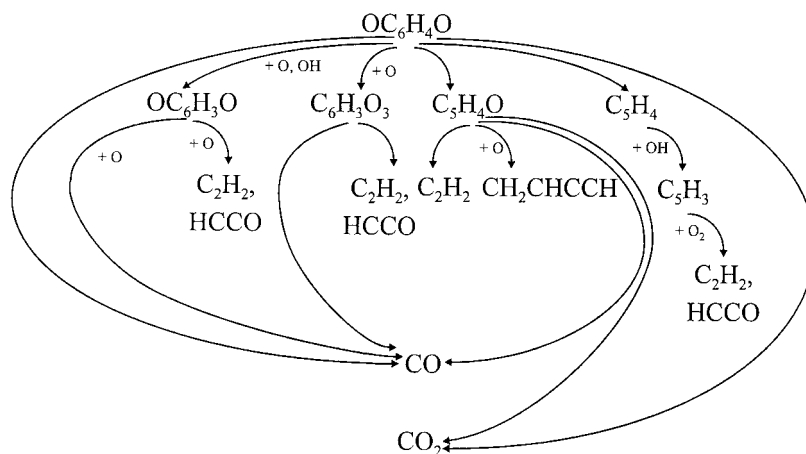


**Figure 8** Reaction path diagram for *p*-benzoquinone oxidation.

is seen that an increase in oxygen concentration results in a shift of the onset of CO<sub>2</sub> formation towards lower temperatures.

The model predictions, carried out with the mechanism in Appendix A, are in good agreement with the experiments. Through analysis of the calculations it is possible to identify the rate limiting processes in the benzoquinone oxidation. Figure 8 shows a reaction pathway diagram for the benzoquinone oxidation.

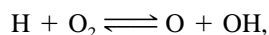
Independent of the oxygen level, OC<sub>6</sub>H<sub>4</sub>O is largely consumed through thermal dissociation at lower temperatures. At the lowest oxygen concentration, thermal decomposition dominates at temperatures up to 1150 K. As the temperature is increased, the radical pool is replenished and reactions between OC<sub>6</sub>H<sub>4</sub>O and the O/H radical pool eventually become significant. At higher temperatures, coinciding with the onset of CO oxidation to CO<sub>2</sub>, these reactions become responsible for a large fraction of the conversion of *p*-benzoquinone. At high oxygen concentrations this shift occurs at lower temperatures, since the presence of O<sub>2</sub> promotes the radical formation.

The interaction of *p*-benzoquinone with the radical pool proceeds mainly through the following reactions:



Subsequently, we assume rapid ring opening of the OC<sub>6</sub>H<sub>3</sub>O and C<sub>6</sub>H<sub>3</sub>O<sub>3</sub> radicals by reaction with the radical pool (R8, R9) or by thermal dissociation (R10). These reactions feed into the C<sub>2</sub> hydrocarbon pool, which is quickly oxidized under the conditions studied. For the O<sub>2</sub> concentration of 4%, this reaction sequence becomes important at temperatures of around 1050 K, while for the low oxygen concentration it becomes significant above 1100 K.

In order to obtain an estimate of the reaction of OC<sub>6</sub>H<sub>4</sub>O with OH, the effects of CO on the oxidation of *p*-benzoquinone were studied. The results are shown in Figure 9. The presence of CO enhances the consumption of OC<sub>6</sub>H<sub>4</sub>O significantly, due to the chain branching sequence



which contributes to replenish the radical pool. As consequence of that, the oxidation regime of *p*-benzoquinone is shifted to lower temperatures, about

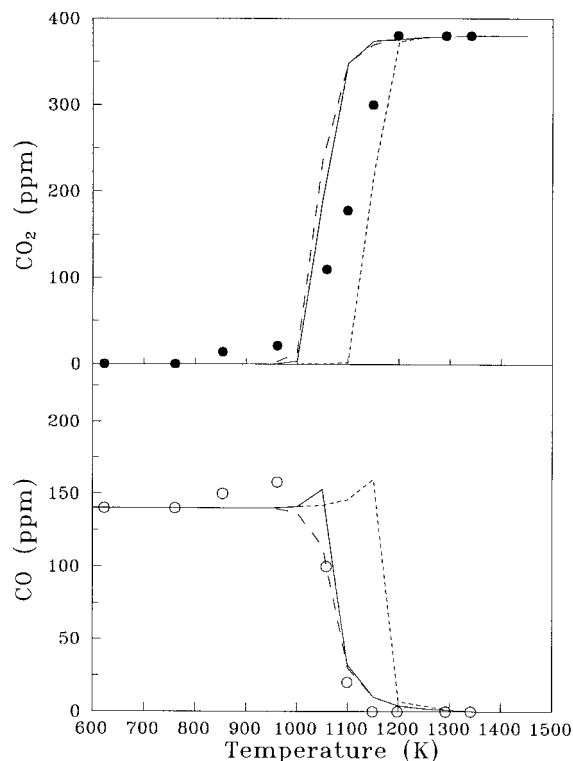


**Figure 9** Comparison of experimental data and model predictions for CO and CO<sub>2</sub> formation in the oxidation of *p*-benzoquinone in presence of CO. Symbols denote experimental data and lines denote model predictions. Inlet concentrations: 40 ppm OC<sub>6</sub>H<sub>4</sub>O; 140 ppm CO; 3.8% O<sub>2</sub>; 1.6% H<sub>2</sub>O; and balance N<sub>2</sub>. Pressure is 1.03 atm. Residence time (s) = 220/*T*(K). Solid lines denote calculations made with the mechanism of the present work. Short dashed lines: calculations made with a rate for reaction (R7) ten times faster than the constant used in the present work. Long dashed lines: calculations made with a rate for reaction (R7) ten times slower than the constant used in the present work.

100 K, compared to the absence of CO. *P*-benzoquinone is completely oxidized at 1100 K under the present reaction conditions. Calculations reveal that the major pathways for OC<sub>6</sub>H<sub>4</sub>O oxidation in the presence of CO are similar to those when CO is absent, even though they occur at lower temperatures.

The competition between parabenzoquinone and carbon monoxide for OH affects the chain branching in the system and thereby the oxidation rate. If the OC<sub>6</sub>H<sub>4</sub>O + OH reaction (R7) is fast, the CO induced chain branching becomes less significant, and the onset of CO oxidation is shifted to higher temperatures. On the other hand, if reaction (R7) is very slow the CO oxidation will be largely unaffected by the presence of OC<sub>6</sub>H<sub>4</sub>O. From the experimental results it is, thus, possible to obtain an estimate of *k*<sub>7</sub>. From the results shown in Figure 9, we have derived a value for

## REACTION MECHANISM

	A	$\beta$	$E_a$	Source
1. $OC_6H_4O \rightleftharpoons C_5H_4O + CO$	3.7E11	0.00	59000	see text
2. $OC_6H_4O \rightleftharpoons C_5H_4 + CO_2$	3.5E12	0.00	67000	see text
3. $OC_6H_4O + H \rightarrow C_5H_5O + CO$	2.5E13	0.00	4700	est, see text
4. $OC_6H_4O + H \rightarrow OC_6H_3O + H_2$	2.0E12	0.00	8100	est, a
5. $OC_6H_4O + O \rightarrow C_6H_3O_3 + H$	1.5E13	0.00	4530	est, a
6. $OC_6H_4O + O \rightarrow OC_6H_3O + OH$	1.4E13	0.00	14700	est, a
7. $OC_6H_4O + OH \rightarrow OC_6H_3O + H_2O$	1.0E06	2.00	4000	see text
8. $OC_6H_3O + H \rightarrow 2C_2H_2 + 2CO$	1.0E14	0.00	0	est
9. $OC_6H_3O + O \rightarrow C_2H_2 + HCCO + 2CO$	1.0E14	0.00	0	est
10. $C_6H_3O_3 \rightarrow C_2H_2 + HCCO + 2CO$	1.0E12	0.00	50000	est
11. $C_5H_5O \rightleftharpoons CH_2CHCHCH + CO$	7.5E11	0.00	43900	[4,12] est
12. $C_5H_4O \rightarrow C_2H_2 + C_2H_2 + CO$	1.0E15	0.00	78000	[4] est
13. $C_5H_4O + H \rightarrow CH_2CHCCH_2 + CO$	2.5E13	0.00	4700	est, $k_3$
14. $C_5H_4O + O \rightarrow CH_2CHCCH + CO_2$	1.0E13	0.00	2000	est
15. $C_5H_4 + H \rightleftharpoons C_5H_3 + H_2$	1.0E06	2.50	5000	est, b
16. $C_5H_4 + O \rightleftharpoons C_5H_3 + H_2$	1.0E06	2.50	3000	est, b
17. $C_5H_4 + OH \rightleftharpoons C_5H_3 + H_2O$	1.0E07	2.00	0	est, b
18. $C_5H_3 + O_2 \rightleftharpoons C_2H_2 + HCCO + CO$	1.0E12	0.00	0	est, b
19. $CH_2CHCHCH(+M) = CH_2CHCCH + H(+M)$	1.0E14	0.00	37000	[32]
Low pressure limit:	1.0E14	0.00	30000	
Enhanced third-body efficiencies: $H_2O=5$				
20. $CH_2CHCHCH + H \rightleftharpoons CH_2CHCCH_2 + H$	1.0E14	0.00	0	[32]
21. $CH_2CHCHCH + H \rightleftharpoons CH_2CHCCH + H_2$	3.0E07	2.00	1000	[32]
22. $CH_2CHCHCH + OH \rightleftharpoons CH_2CHCCH + H_2O$	2.0E07	2.00	1000	[32]
23. $CH_2CHCHCH + O_2 \rightarrow C_2H_2 + CH_2O + HCO$	1.0E12	0.00	0	est
24. $CH_2CHCCH_2(+M) = CH_2CHCCH + H(+M)$	1.0E14	0.00	50000	[32]
Low pressure limit:	2.0E15	0.00	42000	
Enhanced third-body efficiencies: $H_2O=5$				
25. $CH_2CHCCH_2 + H \rightleftharpoons CH_3 + H_2CCCH$	1.0E14	0.00	0	[32]
26. $CH_2CHCCH_2 + OH \rightleftharpoons CH_2CHCCH + H_2O$	3.0E13	0.00	0	[32]
27. $CH_2CHCCH + H \rightleftharpoons HCCHCCH + H_2$	2.0E07	2.00	15000	[32]
28. $CH_2CHCCH + H \rightleftharpoons H_2CCCCH + H_2$	3.0E07	2.00	5000	[32]
29. $CH_2CHCCH + OH \rightleftharpoons HCCHCCH + H_2O$	7.5E06	2.00	5000	[32]
30. $CH_2CHCCH + OH \rightleftharpoons H_2CCCCH + H_2O$	1.0E07	2.00	2000	[32]
31. $HCCHCCH(+M) \rightleftharpoons C_4H_2 + H(+M)$	1.0E14	0.00	36000	[32]
Low pressure limit:	1.0E14	0.00	30000	
Enhanced third-body efficiencies: $H_2O=5$				
32. $HCCHCCH + H \rightleftharpoons H_2CCCCH + H$	1.0E14	0.00	0	[32]
33. $HCCHCCH + OH \rightleftharpoons C_4H_2 + H_2O$	1.0E13	0.00	0	est

**Appendix A** Mechanism Subset Describing the Oxidation of  $C_3$ – $C_6$  Hydrocarbons. Rate Constants are Expressed as  $k = AT^{\beta}\exp(-E_A/RT)$ . Units are cal,  $cm^3$ , mole, and sec

## REACTION MECHANISM (con't)

34.	$H_2CCCCH(+M) \rightleftharpoons C_4H_2 + H(+M)$	1.0E14	0.00	55000	[32]
	Low pressure limit:	2.0E15	0.00	48000	
	Enhanced third-body efficiencies:				
	$H_2O=5$				
35.	$H_2CCCCH + H \rightleftharpoons C_4H_2 + H_2$	5.0E13	0.00	0	[32]
36.	$H_2CCCCH + O \rightleftharpoons CH_2CO + C_2H$	2.0E13	0.00	0	[32]
37.	$H_2CCCCH + O \rightleftharpoons H_2C_4O + H$	2.0E13	0.00	0	[32]
38.	$H_2CCCCH + OH \rightleftharpoons C_4H_2 + H_2O$	3.0E13	0.00	0	[32]
39.	$H_2CCCCH + O_2 \rightleftharpoons CH_2CO + HCCO$	1.0E12	0.00	0	[32]
40.	$H_2CCCCH + CH_2 \rightleftharpoons C_3H_4 + C_2H$	2.0E13	0.00	0	[32]
41.	$C_4H_2 + H \rightleftharpoons C_4H + H_2$	2.0E07	2.00	2000	[32]
42.	$C_4H_2 + O \rightleftharpoons C_3H_2 + CO$	1.2E12	0.00	0	[32]
43.	$C_4H_2 + OH \rightleftharpoons H_2C_4O + H$	6.7E12	0.00	-410	[32]
44.	$C_4H_2 + OH \rightleftharpoons C_4H + H_2O$	1.0E07	2.00	1000	[32]
45.	$H_2C_4O + H \rightleftharpoons C_2H_2 + HCCO$	5.0E13	0.00	3000	[32]
46.	$H_2C_4O + OH \rightleftharpoons CH_2CO + HCCO$	1.0E07	2.00	2000	[32]
47.	$C_4H + O_2 \rightleftharpoons CO + CO + C_2H$	1.0E13	0.00	0	[32]
48.	$C_3H_4 + H \rightleftharpoons C_3H_4P + H$	1.0E13	0.00	5000	[32]
49.	$C_3H_4 + H \rightleftharpoons H_2CCCH + H_2$	3.0E07	2.00	5000	[32]
50.	$C_3H_4 + OH \rightleftharpoons H_2CCCH + H_2O$	2.0E07	2.00	1000	[32]
51.	$C_3H_4P + H \rightleftharpoons H_2CCCH + H_2$	3.0E07	2.00	5000	[32]
52.	$C_3H_4P + H \rightleftharpoons CH_3 + C_2H_2$	1.0E14	0.00	4000	[32]
53.	$C_3H_4P + OH \rightleftharpoons H_2CCCH + H_2O$	2.0E07	2.00	1000	[32]
54.	$H_2CCCH + H(+M) \rightleftharpoons C_3H_4(+M)$	1.0E17	-0.82	315	[32]
	Low pressure limit:	3.5E55	-4.88	2225	
	Troe parameters: 0.7086 134 1784 5740				
	Enhanced third-body efficiencies:				
	$H_2O=8.6$				
55.	$H_2CCCH + H(+M) \rightleftharpoons C_3H_4P(+M)$	1.0E17	-0.82	315	[32]
	Low pressure limit:	3.5E55	-4.88	2225	
	Troe parameters: 0.7086 134 1784 5740				
	Enhanced third-body efficiencies:				
	$H_2O=8.6$				
56.	$H_2CCCH + H \rightleftharpoons C_3H_2 + H_2$	5.0E13	0.00	1000	[32]
57.	$H_2CCCH + O \rightleftharpoons CH_2O + C_2H$	1.4E14	0.00	0	[32]
58.	$H_2CCCH + OH \rightleftharpoons C_3H_2 + H_2O$	2.0E13	0.00	0	[32]
59.	$H_2CCCH + O_2 \rightleftharpoons CH_2CO + HCO$	3.0E10	0.00	2868	[32]
60.	$C_3H_2 + O \rightleftharpoons C_2H_2 + CO$	1.0E14	0.00	0	[32]
61.	$C_3H_2 + OH \rightleftharpoons C_2H_2 + HCO$	5.0E13	0.00	0	[32]
62.	$C_3H_2 + O_2 \rightleftharpoons HCCO + CO + H$	2.0E12	0.00	1000	[32]

a: Estimated as  $\frac{2}{3}$  of the corresponding reaction of  $C_6H_6$

b: Estimated by an isoelectronic analogy with the corresponding reaction of  $C_3H_8$

Appendix A (Continued)

## Thermodynamic properties for selected species

Species	$\Delta H_{f298}$	$S_{298}$	$C_{p300}$	$C_{p400}$	$C_{p500}$	$C_{p600}$	$C_{p800}$	$C_{p1000}$	$C_{p1500}$	Source
OC <sub>6</sub> H <sub>4</sub> O	-29.37	79.62	26.04	32.20	37.67	42.27	48.87	53.42	59.48	[34]
C <sub>5</sub> H <sub>5</sub> O	43.35	71.37	21.16	27.44	32.67	37.00	43.54	47.98	54.07	[4]
C <sub>5</sub> H <sub>4</sub> O	-1.59	66.49	19.70	25.79	30.69	34.62	40.25	43.90	49.00	[34]
C <sub>5</sub> H <sub>4</sub>	111.07	70.89	20.93	25.14	28.52	31.23	35.29	38.35	42.92	[34]
CH <sub>2</sub> CHCHCH	86.09	73.06	19.38	23.47	27.21	30.54	35.76	38.89	43.16	[32,33]
CH <sub>2</sub> CHCCH <sub>2</sub>	74.14	75.31	19.49	23.12	26.47	29.48	34.32	37.37	41.84	[32,33]
CH <sub>2</sub> CHCCH	69.14	67.33	17.32	20.61	23.62	26.30	30.53	33.20	37.25	[32,33]
HCCHCCH	129.88	69.06	18.02	20.82	23.29	25.41	28.56	30.46	33.46	[32,33]
H <sub>2</sub> CCCCH	111.32	72.94	20.24	22.43	24.44	26.23	29.10	30.93	33.68	[32,33]
C <sub>4</sub> H <sub>2</sub>	111.70	59.77	17.74	20.03	21.85	23.24	25.10	26.61	28.96	[32,33]
C <sub>4</sub> H	155.08	60.89	14.10	15.37	16.56	17.66	19.59	21.15	23.44	[32,33]
H <sub>2</sub> C <sub>4</sub> O	54.59	66.43	17.27	19.62	21.79	23.73	26.81	28.73	31.51	[32,33]
C <sub>3</sub> H <sub>4</sub>	47.63	57.94	14.25	16.97	19.46	21.71	25.45	28.20	32.06	[32,33]
C <sub>3</sub> H <sub>4</sub> P	45.77	58.89	14.51	17.06	19.40	21.54	25.16	27.90	31.79	[32,33]
H <sub>2</sub> CCCH	83.04	61.48	15.84	17.74	19.47	21.01	23.43	25.00	27.55	[32,33]
C <sub>3</sub> H <sub>2</sub>	129.60	64.81	14.93	16.10	16.91	17.55	18.72	19.74	21.22	[32,33]

**Appendix B** Thermodynamic Properties for Selected Species. Units are cal, mole, and Kelvin

$k_7$  of  $1.5 \cdot 10^{11}$  cm<sup>3</sup>/mole-s at 1075 K. Unfortunately, the observed CO and CO<sub>2</sub> profiles are only sensitive to this competition in a fairly narrow temperature range between 1000 and 1100 K. This fact, together with uncertainties in the reaction mechanism used, limits the accuracy of this determination. The model predictions shown as solid lines in Figure 9 are carried out with an extrapolated value for  $k_7$  of  $1.0 \cdot 10^6 \cdot T^2 \exp(-2000/T)$  cm<sup>3</sup>/mole-s. The sensitivity of the results to the rate of this reaction is also seen in Figure 9, where calculations with a reaction rate 10 times faster (short-dashed lines) and slower (long-dashed lines) are represented.

## CONCLUSION

A combined experimental study of the pyrolysis and oxidation of parabenzquinone has been performed in the temperature range 600–1500 K. A detailed reaction mechanism for oxidation and pyrolysis of para-

benzoquinone has been proposed, which provides a good description of the experimental results obtained in this work.

A key issue in the pyrolysis and oxidation of parabenzquinone is the branching fraction between the dissociation channels  $OC_6H_4O \rightleftharpoons C_5H_4O + CO$ , and  $OC_6H_4O \rightleftharpoons C_5H_4 + CO_2$ , and the fate of C<sub>5</sub>H<sub>4</sub>O. Our results indicate that an intramolecular channel to CO<sub>2</sub> is active, increasing in importance with temperature. However, the data interpretation depends on assumptions of thermal stability and dissociation products for C<sub>5</sub>H<sub>4</sub>O as well as the potential importance of dimerization of this species.

Under oxidizing conditions and at high temperatures, the interaction between parabenzquinone and the radical pool becomes significant. Under the present conditions, the most important step is the H abstraction by reaction with OH, leading to the OC<sub>6</sub>H<sub>3</sub>O radical with subsequent ring opening.

The experimental and theoretical work presented here constitute the first systematic study of paraben-

zoquinone chemistry. Parabenzoquinone may be important intermediate species in the oxidation of aromatic compounds such as benzene, and the results obtained extend the knowledge of parabenzoquinone behavior under pyrolysis and oxidation conditions.

The work is carried out as part of the combustion research programs at the Department of Chemical and Environmental Engineering of the University of Zaragoza and at the Department of Chemical Engineering of the Technical University of Denmark (CHEC). The CHEC research program is cofunded by the Danish Technical Research Council, Elsam, Elkraft, and the Danish Ministry of Energy. The authors wish to thank Dr. J. Ruiz for his help with the flash-pyrolysis experiment, and Dr. P. Frank for helpful discussions concerning *p*-benzoquinone pyrolysis.

## BIBLIOGRAPHY

- J. D. Bittner and J. B. Howard, *Eighteenth Symposium (Int.) on Combustion*, The Combustion Institute, Pittsburgh, Pennsylvania, 1981, p. 1105.
- C. Venkat, K. Brezinsky, and I. Glassman, *Nineteenth Symposium (Int.) on Combustion*, The Combustion Institute, Pittsburgh, Pennsylvania, 1982, p. 143.
- K. Brezinsky, *Prog. Energy Combust. Sci.*, **12**, 1 (1986).
- J. L. Emdee, K. Brezinsky, and I. Glassman, *J. Phys. Chem.* **96**, 2151 (1992).
- R. P. Lindstedt and G. Skevis, *Combust. Flame* **99**, 551 (1994).
- H.-Y. Zhang and J. T. McKinnon, *Combust. Sci. Techn.* **107**, 261 (1995).
- R. P. Lindstedt and L. Q. Maurice, *Combust. Sci. Techn.* **120**, 119 (1996).
- Y. Tan and P. Frank, *Twenty-Sixth Symposium (Int.) on Combustion*, The Combustion Institute, Pittsburgh, Pennsylvania, 1996, p. 677.
- S. G. Davis, H. Wang, K. Brezinsky, and C. K. Law, *Twenty-Sixth Symposium (Int.) on Combustion*, The Combustion Institute, Pittsburgh, Pennsylvania, 1996, p. 1025.
- D. L. Baulch, C. J. Cobos, R. A. Cox, Th. Just, J. A. Kerr, M. J. Pilling, J. Troe, R. W. Walker, and J. Warnatz, *J. Phys. Chem. Ref. Data* **21**, 411 (1992).
- D. L. Baulch, C. J. Cobos, R. A. Cox, P. Frank, G. Hayman, Th. Just, J. A. Kerr, T. Murrells, M. J. Pilling, J. Troe, R. W. Walker, and J. Warnatz, *J. Phys. Chem. Ref. Data* **23**, 847 (1994).
- P. Frank, J. Herzler, Th. Just, and C. Wahl, *Twenty-Fifth Symposium (Int.) on Combustion* The Combustion Institute, Pittsburgh, Pennsylvania, 1994, p. 833.
- S. S. Kumaran and J. V. Michael, *Proceedings of the 21st Int. Symp. on Shock Waves*, Great Keppel Island, Australia, 1997.
- R. Buth, K. Hoyeremann, and J. Seeba, *Twenty-Fifth Symposium (Int.) on Combustion*, The Combustion Institute, Pittsburgh, Pennsylvania, 1994, p. 841.
- B. Dellinger, S. L. Mazer, and R. A. Dobbs, *J. Air Manage. Assoc.* **41**, 838 (1991).
- A. M. Mebel and M. C. Lin, *J. Am. Chem. Soc.* **116**, 9577 (1994).
- M. C. Lin and A. M. Mebel, *J. Phys. Org. Chem.* **8**, 407 (1995).
- H. J. Hageman and U. E. Wiersum, *Tetrahedron Lett.* **45**, 4329 (1971).
- H. J. Hageman and U. E. Wiersum, *Angew. Chem.* **7**, 314 (1972).
- P. de Champlain and P. de Mayo, *Can. J. Chem.* **50**, 270 (1972).
- T. Sakai and M. Hattori, *Chem. Lett.* 1103 (1975).
- T. Sakai and M. Hattori, *Chem. Lett.* 1153 (1976).
- T. Sakai, M. Hattori, and N. Yamane, *J. Japan Petrol. Inst.* **23**, 44 (1980).
- T. Sakai, M. Hattori, and N. Yamane, *J. Japan Petrol. Inst.* **23**, 334 (1980).
- W. D. Gräber and K. J. Hüttinger, *Erdöl Kohle Erdgas Petrochem.* **33**, 416 (1980).
- D. C. de Jongh, R. Y. van Fossen, and C. F. Bourgeois, *Tetrahedron Lett.* **3**, 271 (1967).
- D. C. de Jongh and D. A. Brent, *J. Org. Chem.* **35**, 4204 (1970).
- G.-J. Schraa, I. W. C. E. Arends, and P. Mulder, *Chem. Soc. Perkin Trans.* **2**, 189 (1994).
- P. G. Kristensen, P. Glarborg, and K. Dam-Johansen, *Combust. Flame* **107**, 211 (1996).
- P. Glarborg, M. U. Alzueta, K. Dam-Johansen, and J. A. Miller, *Combust. Flame*, **115**, 1 (1998).
- J. A. Miller and C. F. Melius, *Combust. Flame* **91**, 21 (1992).
- J.-F. Pauwels, J. V. Volponi, and J. A. Miller, *Combust. Sci. Techn.* **110**, 249 (1995).
- R. J. Kee, F. M. Rupley, and J. A. Miller, *The Chemkin Thermodynamic Data Base*, Sandia Report SAND87-8215, Sandia National Laboratories, Livermore, California, 1991.
- A. Burcat and B. McBride, *1995 Ideal Gas Thermodynamic Data for Combustion and Air-Pollution Use*; Aerospace Engineering Report TAE 732, Technion, Israel. Institute of Technology, 1995 and updates.
- J. A. Manion and R. Louw, *J. Phys. Chem.* **94**, 4127 (1990).
- I. W. C. E. Arends, R. Louw, and P. Mulder, *J. Phys. Chem.* **97**, 7914 (1993).
- P. N. Bajaj and A. Fontijn, *Combust. Flame* **105**, 239 (1996).
- R. Atkinson, *Int. J. Chem. Kinet.* **19**, 799 (1987).
- R. Atkinson, S. M. Aschmann, J. Arey, and B. Zielinska, *Atmospheric Environment* **23**, 2679 (1989).
- A. E. Lutz, R. J. Kee, and J. A. Miller, *SENKIN: A Fortran Program for Predicting Homogenous Gas Phase Chemical Kinetics with Sensitivity Analysis*, Sandia Report SAND87-8248, Sandia National Laboratories, Livermore, California, 1987.
- R. J. Lutz, F. M. Rupley, and J. A. Miller, *CHEMKIN-*

- II: A Fortran Chemical Kinetics Package for the Analysis of Gas-Phase Chemical Kinetics*, Sandia Report SAND89-8009, Sandia National Laboratories, Livermore, California, 1989.
42. J. Sauer and R. Sustmann, *Angew. Chem.* **92**, 773 (1980).
  43. J. Arauzo, D. Radlein, J. Piskorz, and D. S. Scott, *Energy Fuels* **8**, 1192 (1994).
  44. J. A. Miller and P. Glarborg, in "Gas-Phase Chemical Reaction Systems; Experiments and Modeling 100 Years after Max Bodenstein", (Eds. J. Wolfrum, H.-R. Volpp, R. Rannacher, J. Warnatz), *Springer Series in Chemical Physics* **61**, 318 (1996).
  45. A. M. Dean and J. W. Bozzelli, "Combustion Chemistry of Nitrogen", *Combustion Chemistry II*, (ed. W. C. Gardiner, Jr.), Springer Verlag, in press (1997).